Borneo Journal of Pharmacy
Vol 9 Issue 2 June 2026
Pages 188 – 197

https://journal.umpr.ac.id/index.php/bjop/article/view/11781
DOI: https://doi.org/10.33084/bjop.v9i2.11781
e-ISSN: 2621-4814

Research Article

Rapid and Controlled: Microflow Reactor-Assisted Synthesis of Cinnamaldehyde and Ethyl Cinnamate along with Their Cytotoxic Activity Against Several Cell Lines

Nindita Fransiska Rahmawati [1]
Muhtadi [1*]
Andi Suhendi [1]
Ahmad Fauzi [1]
Didin Mujahidin [2]
Ahwan [3]
Agustono Wibowo [4]

[1] Department of Pharmacy, Universitas Muhammadiyah Surakarta, Sukoharjo, Central Java, Indonesia
[2] Department of Chemistry, Institut Teknologi Bandung, Bandung, West Java, Indonesia
[3] Faculty of Science, Technology, and Health, Universitas Sahid Surakarta, Surakarta, Central Java, Indonesia
[4] Faculty of Applied Sciences, Universiti Teknologi MARA Pahang, Jengka, Pahang, Malaysia

*email: muhtadi@ums.ac.id; phone: +6282136362763

Keywords:
Cinnamaldehyde synthesis
Cytotoxic activity
Ethyl cinnamate
Green chemistry
Microflow reactor

Abstract

Cinnamaldehyde is a major aromatic compound utilized in the pharmaceutical industry due to its diverse biological activities, including anticancer potential. This study aims to develop a rapid and controlled synthesis method for cinnamaldehyde and ethyl cinnamate using microflow reactor technology, followed by structural elucidation and cytotoxic evaluation against HeLa, MCF-7, and T47D cancer cell lines. The synthesis of cinnamaldehyde was performed via aldol condensation of benzaldehyde and acetaldehyde (1.3:1 molar ratio) at 70°C, while ethyl cinnamate was synthesized through a two-step process involving Pinnick oxidation and Fischer esterification. The results demonstrated that microflow synthesis achieved a cinnamaldehyde yield of 52% with high purity (100% based on HPLC relative area), and ethyl cinnamate with 99% purity. In cytotoxic assays, synthesized cinnamaldehyde exhibited moderate activity, most notably against HeLa cells with an IC_{50} of 95 µg/mL, whereas ethyl cinnamate showed lower potency (IC_{50} > 200 µg/mL). Although the synthesized compounds were less potent than the standard cinnamaldehyde (IC_{50} 1.56 µg/mL) and Doxorubicin control, this study confirms that microflow reactor technology is a highly effective and time-efficient method for producing high-purity cinnamate derivatives.

Received: December 15th, 2025
1st Revised: January 17th, 2026
Accepted: February 18th, 2026
Published: June 30th, 2026

INTRODUCTION

Cinnamaldehyde is an organic compound with the chemical formula $C_6H_5CH{=}CHCHO$ that naturally exists predominantly as the *trans* (*E*) isomer, featuring a characteristic cinnamon aroma[1]. Cinnamaldehyde has broad applications across industrial and pharmaceutical sectors owing to its diverse biomedical properties[2]. Beyond its commercial value, cinnamaldehyde has attracted significant interest in medicinal chemistry due to its biological activities. Although earlier studies primarily evaluated its antibacterial and antidiabetic potential, recent investigations increasingly highlight its promise as an effective anticancer candidate[3].

Despite its therapeutic potential, the accessibility of high-purity cinnamaldehyde in developing nations such as Indonesia is constrained by a high reliance on imported fine chemicals, which account for over 90% of domestic chemical material requirements[4]. Establishing efficient domestic synthesis routes is therefore of strategic importance. However, conventional

How to cite: Rahmawati NF, Muhtadi, Suhendi A, Fauzi A, Mujahidin D, Ahwan, et al. Rapid and Controlled: Microflow Reactor-Assisted Synthesis of Cinnamaldehyde and Ethyl Cinnamate along with Their Cytotoxic Activity Against Several Cell Lines. Borneo J Pharm. 2026;9(2):188-97. doi:10.33084/bjop.v9i2.11781

batch synthesis of cinnamaldehyde via aldol condensation presents major technical challenges. Traditional batch methods are typically hampered by extended reaction times, poor heat-transfer efficiency, and the formation of undesirable side products, such as high-molecular-weight polymers or Cannizzaro disproportionation products. As a consequence, conventional batch processes frequently yield low recovery rates (often reported as 40%-50%) and inconsistent product purity, underscoring the need for more controlled synthetic alternatives[5].

To overcome these synthetic limitations, microflow reactor technology has emerged as an advanced platform for continuous organic synthesis. Unlike bulk batch reactors, microflow systems feature exceptionally high surface-to-volume ratios that facilitate rapid, homogeneous heat and mass transfer[6]. This precise control over reaction parameters, specifically temperature gradients and residence time, enables the rapid and controlled synthesis of sensitive or highly reactive compounds. By minimizing the residence time of unstable intermediates and preventing localized thermal hot spots, microflow reactors effectively suppress side reactions, thereby improving both product selectivity and overall synthetic yield compared to traditional batch methodologies[7].

Although the synthesis of various cinnamaldehyde derivatives has been reported previously, the literature has not comprehensively integrated continuous microflow-assisted synthesis with a comparative evaluation of cytotoxic efficacy across biologically distinct cancer cell lines. This study specifically selects HeLa (cervical carcinoma), MCF-7, and T47D (breast adenocarcinoma) cell lines to evaluate the biological activity of the synthesized compounds. These cell lines were chosen to represent distinct oncological profiles: HeLa cells are highly susceptible to reactive oxygen species (ROS)-inducing agents, whereas MCF-7 and T47D cells differ in their caspase-3 expression and estrogen receptor status. Screening across this panel provides a robust understanding of the cytotoxic efficacy and potential selectivity of these compounds. Therefore, this study aims to develop an efficient, rapid, and sustainable synthesis method for cinnamaldehyde and its derivative, ethyl cinnamate, utilizing microflow reactor technology. This research offers novelty by optimizing continuous-flow synthesis parameters to enhance yield and chemical purity relative to conventional methods, followed by comprehensive structural elucidation and comparative cytotoxic evaluation across multiple cancer cell lines to establish their potential as therapeutic candidates.

MATERIALS AND METHODS

Materials

All chemical reagents and solvents utilized in this study were of analytical grade, sourced from Merck (Darmstadt, Germany) and Sigma-Aldrich (St. Louis, MO, USA), and used without additional chemical purification. The primary chemical materials included cinnamaldehyde reference standard (Sigma-Aldrich), acetaldehyde (Merck), benzaldehyde (Merck), sodium hydroxide (Merck), sodium chlorite (Merck), hydrogen peroxide (Merck), sulfuric acid (Merck), hydrochloric acid (Merck), sodium sulfite (Merck), ethanol (Merck), ethyl acetate (Merck), and anhydrous sodium sulfate (Merck). Biological reagents for cell culture and viability testing comprised Dulbecco's Modified Eagle Medium (DMEM), fetal bovine serum (FBS), penicillin-streptomycin, 3-(4,5-dimethylthiazol-2-yl)-2,5-diphenyltetrazolium bromide (MTT) assay kit, and doxorubicin hydrochloride (Sigma-Aldrich). Continuous-flow organic reactions were conducted using a microflow reactor system managed via an automated Haiwell HMI control interface. Fluid delivery was controlled using a Runze Smart SY01 micro-syringe pump featuring a 5.0 mL internal volume. The microfluidic channel consisted of polytetrafluoroethylene (PTFE) tubing with an overall length of 2.0 m, an internal diameter (ID) of 1.6 mm, and an outer diameter (OD) of 3.2 mm. Optical density measurements for colorimetric bioassays were recorded using a BioRad microplate reader.

Methods

Microflow synthesis of cinnamaldehyde

Cinnamaldehyde was synthesized via a base-catalyzed Claisen-Schmidt aldol condensation between benzaldehyde and acetaldehyde using NaOH as the homogenizing catalyst, as illustrated in **Figure 1**. A liquid mixture of benzaldehyde and acetaldehyde was prepared at a stoichiometric molar ratio of 1.3:1. An excess of benzaldehyde was used to maximize conversion of the limiting acetaldehyde while minimizing self-condensation side reactions. The reactant solution and an

aqueous NaOH catalyst solution were simultaneously delivered into the microreactor inlets using dual syringe pumps at a total volumetric flow rate of 1.0 mL/min. The reaction tubing was immersed in a temperature-controlled bath maintained at 70°C, providing a residence time of 10 minutes[8]. Upon exiting the microreactor outlet, the reaction effluent was immediately collected in a vessel containing chilled 10% dilute H_2SO_4 to quench catalyst activity. The mixture was extracted thrice with ethyl acetate using a separatory funnel. The combined organic phases were dried over Na_2SO_4, filtered, and concentrated under reduced pressure using a rotary evaporator. The crude residue was further purified by column chromatography on silica gel to isolate pure cinnamaldehyde.

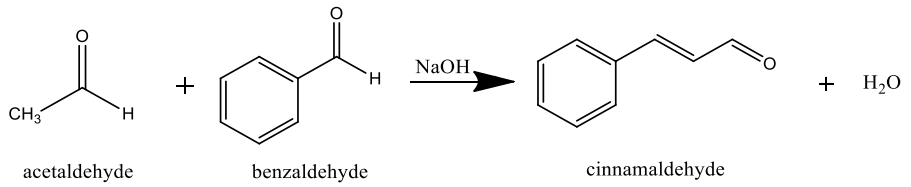

Figure 1. Cinnamaldehyde formation reaction.

Chromatographic purity verification

Chemical purity of the synthesized cinnamaldehyde was initially verified using thin-layer chromatography (TLC) on silica gel 60 F_{254} plates using three distinct mobile phase systems of varying polarities. Chromatograms were developed in chloroform:methanol (9:1 v/v), *n*-hexane:ethyl acetate (8:2 v/v), and toluene:ethyl acetate:methanol (8:1:1 v/v/v)[9]. The detection of a single homogeneous spot under ultraviolet light (254 nm and 365 nm) across all three eluent systems confirmed compound purity. Chromatographic purity was further validated using High-Performance Liquid Chromatography (HPLC) equipped with a C_{18} analytical column (150 x 4.6 mm, 5 µm particle size). The mobile phase comprised an isocratic mixture of methanol and water (85:15 v/v) delivered at a flow rate of 1.0 mL/min, with the column compartment temperature maintained at 29°C. Sample injection volumes were set to 20 µL, and analyte detection was monitored spectrophotometrically at 280 nm[10].

Microflow synthesis of ethyl cinnamate

Ethyl cinnamate was synthesized via a continuous two-step chemical sequence consisting of the oxidation of cinnamaldehyde to cinnamic acid (**Figure 2**), followed by acid-catalyzed Fischer esterification (**Figure 3**). In the first step (Pinnick oxidation), synthesized cinnamaldehyde was oxidized using $NaClO_2$ and H_2O_2. A solution of cinnamaldehyde, aqueous $NaClO_2$, and H_2O_2, mixed in a molar ratio of 1.0:1.7:1.3, was pumped through the microflow reactor at a total flow rate of 1.0 mL/min and a controlled temperature of 10°C, yielding a residence time of 10 minutes. The reactor effluent was treated with aqueous sodium sulfite (Na_2SO_3) to quench residual oxidants, then acidified with 10% HCl to pH 2.0. The acidified mixture was chilled to induce complete crystallization, and the resulting solid cinnamic acid precipitate was recovered by vacuum filtration, washed with cold distilled water, and dried to constant weight. In the second step (Fischer esterification), the purified cinnamic acid was esterified with absolute ethanol in the presence of concentrated H_2SO_4 as a catalyst at a molar ratio of 1.0:3.0 (cinnamic acid to ethanol). The homogeneous mixture was delivered through the microreactor channel at a flow rate of 1.0 mL/min while maintaining the reaction temperature between 70°C and 90°C[11]. The exiting stream was collected, diluted with ethyl acetate, washed with saturated sodium bicarbonate solution and water, and the organic phase was dried over anhydrous Na_2SO_4. Solvent removal under reduced pressure yielded pure ethyl cinnamate.

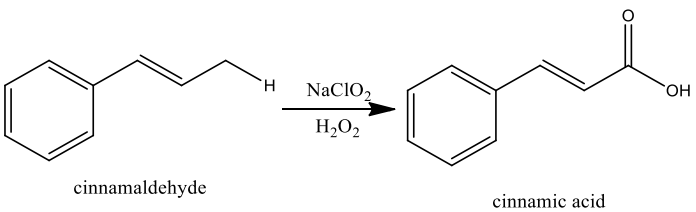

Figure 2. Cinnamaldehyde oxidation reaction.

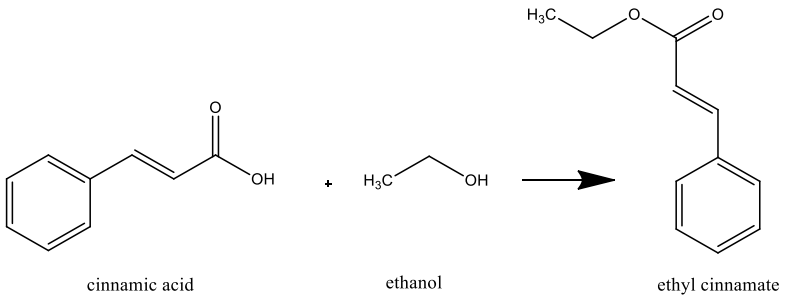

Figure 3. Cinnamic acid esterification reaction.

Spectroscopic characterization and structural elucidation

Fourier-Transform Infrared (FTIR) spectra were recorded on an FTIR spectrophotometer operating in KBr mode across a wavenumber range of 4000 to 400 cm^{-1} at a resolution of 4 cm^{-1} to identify diagnostic functional groups[12]. Nuclear Magnetic Resonance (NMR) spectra were acquired on a spectrometer operating at 500 MHz for ^{1}H-NMR and 125 MHz for ^{13}C-NMR at 25°C. Synthesized samples (10 to 20 mg) were dissolved in 0.6 mL of deuterated chloroform ($CDCl_3$) containing tetramethylsilane (TMS) as an internal chemical shift reference (0.0 ppm). Chemical shift assignments (in ppm), coupling constants (J in Hz), and spin-spin splitting patterns were evaluated to establish full structural elucidation and confirm proton-proton and proton-carbon connectivity[13].

In vitro cytotoxicity bioassay (MTT method)

The *in vitro* cytotoxic activities of cinnamaldehyde and ethyl cinnamate were evaluated against HeLa (human cervical carcinoma), MCF-7 (human breast adenocarcinoma, caspase-3-deficient, ER+), and T47D (human breast ductal carcinoma, caspase-3+/ER+) cell lines using the colorimetric MTT assay, with doxorubicin serving as the positive control. Cells were cultured in high-glucose DMEM supplemented with 10% FBS, 100 U/mL penicillin, and 100 µg/mL streptomycin in a humidified incubator at 37°C under a 5% CO_2 atmosphere. Monolayer cells in the exponential growth phase were harvested, seeded into 96-well microplates at a density of 1 x 10^4 cells/well, and allowed to adhere for 24 hours. Cells were subsequently treated with serial concentrations of test compounds dissolved in DMSO (final DMSO concentration <0.1% v/v) for 24 hours. Following incubation, 20 µL of MTT reagent (5 mg/mL in PBS) was added to each well, and the microplates were incubated for an additional 4 hours at 37°C to allow viable mitochondrial succinate dehydrogenase to convert the tetrazolium salt into insoluble purple formazan crystals. The supernatant culture medium was carefully aspirated, and 100 µL of DMSO was added to each well to solubilize the formazan product. Optical densities were measured at 570 nm using a Bio-Rad microplate reader.

Data analysis

All chemical synthesis experiments and *in vitro* cytotoxicity bioassays were performed in triplicate (n = 3), and quantitative data were expressed as mean ± standard deviation. The half-maximal inhibitory concentration (IC_{50}), defined as the compound concentration required to inhibit cell growth by 50% relative to vehicle controls, was derived from nonlinear regression analysis of dose-response curves that plot percentage cell viability against logarithmic compound concentration. Statistical analyses were performed using SPSS. Significant differences across cell lines and treatment groups were evaluated using one-way Analysis of Variance (ANOVA), followed by Tukey's post hoc multiple comparisons test, with statistical significance set at $p < 0.05$.

RESULTS AND DISCUSSION

The synthesis of cinnamaldehyde was performed via a crossed-aldol condensation between benzaldehyde and acetaldehyde, catalyzed by NaOH. The reaction proceeds via base-mediated abstraction of an α-proton from acetaldehyde, forming a nucleophilic enolate that subsequently attacks the carbonyl carbon of benzaldehyde. This step generates a β-hydroxy aldehyde intermediate, which undergoes thermal dehydration to construct the conjugated enone framework of cinnamaldehyde.

As presented in **Table I**, continuous-flow synthesis produced an average product mass of 13.80 g across three independent runs, corresponding to an isolated chemical yield of 52%. Although microflow technology provides superior heat and mass transfer, thereby minimizing competitive side reactions, the moderate isolated yield suggests minor material losses during post-synthetic downstream purification, specifically solvent extraction and vacuum column chromatography. Furthermore, despite precise reaction control within the microfluidic channel, minor side reactions, such as the Cannizzaro disproportionation of benzaldehyde or oligomerization of the reactive α,β-unsaturated aldehyde, occurred to a limited extent under strongly basic conditions. Nevertheless, the continuous-flow platform significantly reduced the required reaction time to 10 minutes, offering a substantial efficiency advantage over conventional batch methods that typically require multiple hours.

Table I. Results of cinnamaldehyde synthesis.

Experimental Batch	Weight of Synthesized Product (g)
Cinnamaldehyde synthesis (Batch 1)	13.09
Cinnamaldehyde synthesis (Batch 2)	13.80
Cinnamaldehyde synthesis (Batch 3)	14.51
Average Product Mass	13.80

Purity evaluation via TLC across three solvent systems of varying polarities revealed single, symmetrical spots with Rf values identical to those of the reference standards, confirming high chemical purity (**Table II**). The HPLC analysis (**Figure 4**) demonstrated a sharp primary peak at a retention time of 2.27 minutes. The minor deviation (0.08 min) compared to the reference standard (2.35 min) falls within acceptable chromatographic variance and is attributable to slight fluctuations in system backpressure or eluent composition. The complete absence of secondary peak shoulders confirms a relative chromatographic purity of 100% for the isolated cinnamaldehyde[14].

Table II. Results of cinnamaldehyde purity analysis from synthesized product using TLC.

Mobile Phase System	Analytical Parameter	Observed Rf Value
Chloroform : Methanol (9.5:0.5 v/v)	Rf reference standard	0.90
	Rf synthesized cinnamaldehyde	0.90
n-hexane : Ethyl acetate (8.0:2.0 v/v)	Rf reference standard	0.64
	Rf synthesized cinnamaldehyde	0.69
Toluene : Ethyl acetate : Methanol (8.0:1.0:1.0 v/v)	Rf reference standard	0.79
	Rf synthesized cinnamaldehyde	0.76

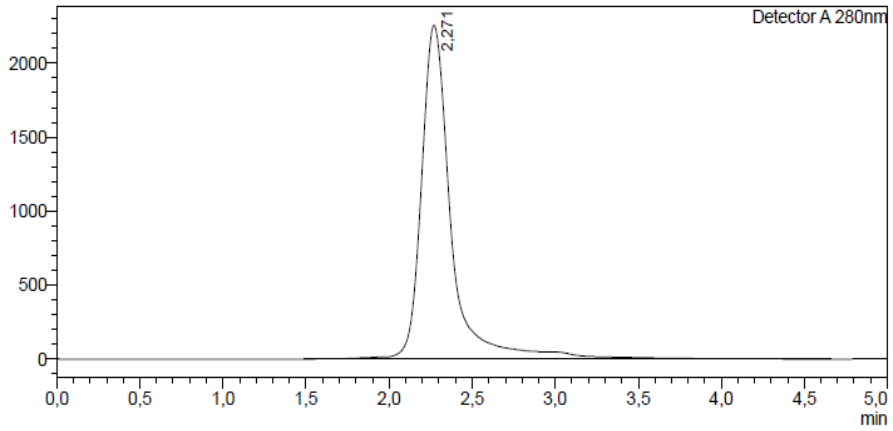

Figure 4. HPLC analysis of cinnamaldehyde.

Structural assignment was confirmed through detailed ^{1}H-NMR and ^{13}C-NMR and FTIR spectroscopy. ^{1}H-NMR ($CDCl_3$, 500 MHz): δ 9.95 (d, 1H, J = 7.8 Hz, -CHO), 7.78 (d, 1H, J = 16.0 Hz, -CH=CH-Ph), 7.50 (d, 1H, J = 16.0 Hz, -CH=CH-CHO), 7.60–7.65 (m, 5H, Ar-H). Minor trace solvent residual signals were detected at δ 1.20 and 4.00–4.10 ppm. ^{13}C-NMR ($CDCl_3$, 125 MHz): δ 192.5 (C=O, -CHO), 137.0 (Cα, -CH=CH-CHO), 134.5 (Cβ, -CH=CH-Ph), 134.5, 129.8, 129.1 (Ph-C). Minor trace residual signals were observed at δ 14.29, 21.16, 60.50, and 171.30 ppm. FTIR (KBr, ν_{max}, cm^{-1}): 3099, 3088, 3064 (aromatic C-H stretching); 3007, 2998, 2983, 2956, 2943, 2851 (aliphatic C-H stretching); 2823, 2737 (aldehyde C-H Fermi doublets); 1734,

1718, 1696 (conjugated carbonyl C=O stretching); 1637, 1627, 1617 (alkene C=C stretching); 1600, 1584, 1577 (aromatic ring C=C stretching); 1456, 1419 (C-H bending); 1311, 1243 (C-C/C-O stretching); 827, 811, 796, 744, 714, 687 (out-of-plane aromatic C-H bending).

In the ^{1}H-NMR spectrum, three diagnostic proton environments confirmed the cinnamaldehyde core: a doublet at δ 9.95 ppm (J = 7.8 Hz) characteristic of the aldehyde proton (-CHO); a complex multiplet at δ 7.60–7.65 ppm corresponding to five aromatic protons on the phenyl ring; and doublets at δ 7.50 and 7.78 ppm with large trans-coupling constants (J = 16.0 Hz) confirming the (*E*)-stereochemistry of the vinylic protons (-CH=CH-). In the ^{13}C-NMR spectrum, the downfield resonance at δ 192.5 ppm corresponds to the conjugated aldehyde carbonyl carbon, while peaks at δ 137.0 and 134.5 ppm confirm the α,β-unsaturated vinylic carbons (Cα and Cβ). Aromatic carbons resonated between δ 129.1 and 134.5 ppm. FTIR spectra verified these features, displaying characteristic aldehyde Fermi resonance doublets at 2823 and 2737 cm^{-1} alongside intense conjugated carbonyl (C=O) absorption at 1734–1696 cm^{-1} and alkene (C=C) stretching at 1637–1617 cm^{-1}.

Ethyl cinnamate was synthesized via a continuous two-stage sequence: Pinnick oxidation of cinnamaldehyde to cinnamic acid followed by acid-catalyzed Fischer esterification. Pinnick oxidation was performed using $NaClO_2$ and H_2O_2 in a microreactor at 10°C with a 10-minute residence time (1.0 mL/min flow rate). In this reaction, H_2O_2 acts as a HOCl scavenger to prevent unwanted aromatic chlorination or double-bond addition, ensuring selective oxidation of the aldehyde group to the carboxylic acid[15,16]. Controlled microfluidic parameters permitted high conversion and selectivity without requiring transition-metal catalysts[17,18]. The resulting intermediate, cinnamic acid, was isolated as white crystals and confirmed to be pure by single-spot TLC. Subsequent Fischer esterification of cinnamic acid with absolute ethanol (1.0:3.0 molar ratio) was catalyzed by H_2SO_4 at 70°C–90°C in the microreactor[19]. Acidic protonation of the carbonyl oxygen enhanced its electrophilicity toward nucleophilic attack by ethanol, producing pale yellow ethyl cinnamate with an average batch mass of 2.08 g (**Table III**).

Table III. Results of ethyl cinnamate synthesis.

Experimental Batch	Weight of Synthesized Product (g)
Ethyl cinnamate synthesis (Batch 1)	2.10
Ethyl cinnamate synthesis (Batch 2)	2.05
Ethyl cinnamate synthesis (Batch 3)	2.08
Average Product Mass	2.08

Comparative TLC analysis (**Table IV**) showed clear Rf shifts between the starting cinnamic acid and ethyl cinnamate, confirming complete esterification. In non-polar mobile phase systems (*n*-hexane:ethyl acetate 7.0:3.0 v/v), ethyl cinnamate exhibited higher Rf values (0.59) than cinnamic acid (0.53), consistent with its reduced polarity and lower affinity for polar silica stationary phases[20]. HPLC analysis of synthesized ethyl cinnamate (**Figure 5**) showed a sharp primary retention peak at 2.0 minutes with a relative peak area of 99%, confirming high chemical purity, alongside a minor trace impurity peak at 2.9 minutes.

Table IV. TLC Analysis results of cinnamic acid and ethyl cinnamate.

Mobile Phase System	Analyte	Observed Rf Value
Chloroform : Methanol (9.0:1.0 v/v)	Cinnamic acid	0.57
	Ethyl cinnamate	0.70
Dichloromethane : Ethyl acetate (8.0:2.0 v/v)	Cinnamic acid	0.69
	Ethyl cinnamate	0.64
n-hexane : Ethyl acetate (7.0:3.0 v/v)	Cinnamic acid	0.53
	Ethyl cinnamate	0.59

Structural verification of ethyl cinnamate was established via NMR and FTIR spectroscopy. ^{1}H-NMR ($CDCl_3$, 500 MHz): δ 7.50 (d, 1H, J = 16.0 Hz, -CH=CH-COOEt), 7.39–7.54 (m, 5H, Ar-H), 6.45 (d, 1H, J = 16.0 Hz, Ph-CH=CH-), 4.27 (q, 2H, J = 7.1 Hz, -OCH_2CH_3), 1.20 (t, 3H, J = 7.1 Hz, -OCH_2CH_3). ^{13}C-NMR ($CDCl_3$, 125 MHz): δ 166.7 (C=O, ester), 145.2 (Cα, Ph-CH=), 118.7 (Cβ, -CH=COOEt), 128.0–133.0 (aromatic carbons), 60.5 (-OCH_2CH_3), 14.2 (-CH_3, ethyl). FTIR (KBr, ν_{max}, cm^{-1}): 3066–3020 (aromatic/alkenic C-H stretching); 2951–2871 (aliphatic C-H stretching); 1717–1704 (ester carbonyl C=O stretching); 1693–1643 (conjugated C=C stretching); 1317–1272 and 1173–1119 (ester C-O stretching); 716 (out-of-plane aromatic C-H bending). The ^{1}H-NMR spectrum displayed diagnostic ethyl ester resonances: a two-proton quartet at δ 4.27 ppm (J = 7.1 Hz, -OCH_2CH_3) and a three-proton triplet at δ 1.20 ppm (J = 7.1 Hz, -OCH_2CH_3). Vinylic doublets appeared at δ 6.45 and

7.50 ppm (J = 16.0 Hz), confirming trans-alkene geometry. In the ^{13}C-NMR spectrum, conversion of the aldehyde to an ester was confirmed by the upfield shift of the carbonyl carbon from δ 192.5 ppm to δ 166.7 ppm, alongside new aliphatic ester carbon signals at δ 60.5 and 14.2 ppm. FTIR spectra further verified ester formation via the disappearance of aldehyde C–H Fermi doublets (2823, 2737 cm^{-1}) and the appearance of strong ester C=O stretching at 1717–1704 cm^{-1} combined with asymmetric C-O stretching at 1317–1272 and 1173–1119 cm^{-1}.

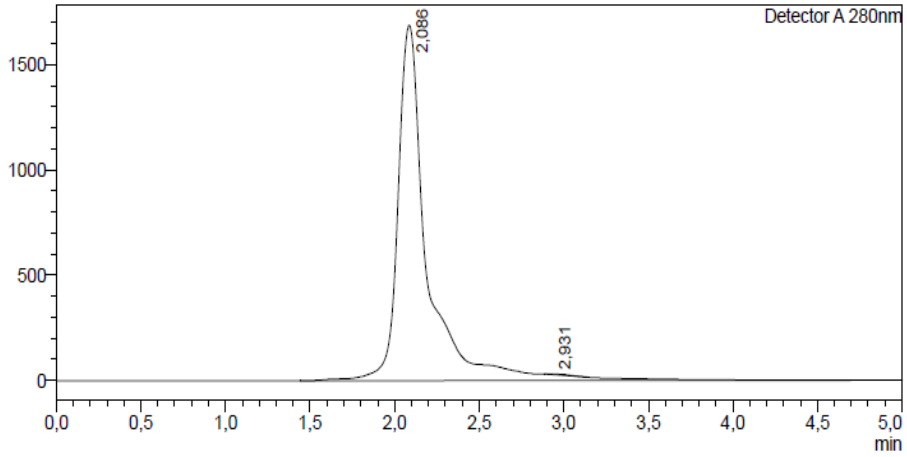

Figure 5. HPLC analysis of ethyl cinnamate.

The cytotoxic potency of the synthesized cinnamaldehyde and ethyl cinnamate was evaluated against the HeLa, MCF-7, and T47D cell lines using the colorimetric MTT assay, and their activities were compared with those of commercial cinnamaldehyde and doxorubicin (**Tables V** to **VII**). Doxorubicin exhibited exceptional cytotoxic potency across all three cell lines (IC_{50} = 0.14 µg/mL in HeLa; 1.37 µg/mL in MCF-7; 0.16 µg/mL in T47D), functioning via DNA intercalation and NADPH/cytochrome P450 reductase-mediated ROS generation[21]. Commercial cinnamaldehyde standard similarly displayed strong antiproliferative activity (IC_{50} = 1.56 µg/mL in HeLa; 9.81 µg/mL in MCF-7; 26.20 µg/mL in T47D), consistent with established mechanisms wherein cinnamaldehyde triggers mitochondrial membrane permeability transition (MPT), ROS accumulation, and cytochrome c release[22]. Synthesized cinnamaldehyde demonstrated notable cytotoxic activity, yielding IC_{50} values of 95.00 µg/mL in HeLa (strong category), 220.00 µg/mL in MCF-7 (moderate category), and 182.00 µg/mL in T47D cells (moderate category)[23]. Synthesized ethyl cinnamate exhibited moderate antiproliferative effects across the panel (IC_{50} = 207.00 µg/mL in HeLa; 438.00 µg/mL in MCF-7; 368.00 µg/mL in T47D).

Table V. IC_{50} values of test compounds against HeLa cell line.

Test Sample	IC_{50} Value (µg/mL)	Cytotoxicity Category
Doxorubicin (positive control)	0.14	Very Strong
Standard cinnamaldehyde	1.56	Very Strong
Synthesized cinnamaldehyde	95.00	Strong
Synthesized ethyl cinnamate	207.00	Moderate

Table VI. IC_{50} values of test compounds against MCF-7 cell line.

Test Sample	IC_{50} Value (µg/mL)	Cytotoxicity Category
Doxorubicin (positive control)	1.37	Very Strong
Standard cinnamaldehyde	9.81	Very Strong
Synthesized cinnamaldehyde	220.00	Moderate
Synthesized ethyl cinnamate	438.00	Moderate

Table VII. IC_{50} values of test compounds against T47D cell line.

Test Sample	IC_{50} Value (µg/mL)	Cytotoxicity Category
Doxorubicin (positive control)	0.16	Very Strong
Standard cinnamaldehyde	26.20	Very Strong
Synthesized cinnamaldehyde	182.00	Moderate
Synthesized ethyl cinnamate	368.00	Moderate

Across all tested cinnamate derivatives, HeLa cells displayed the highest vulnerability to growth inhibition (HeLa > T47D > MCF-7). This differential sensitivity reflects inherent biological variations in intracellular ROS regulation, basal antioxidant enzyme profiles, and the integrity of apoptotic pathways. Cinnamaldehyde primarily induces apoptosis via ROS-mediated mitochondrial collapse[24]. Consequently, cell lines with heightened susceptibility to oxidative stress demonstrate greater sensitivity. MCF-7 cells carry a deletion in the *CASP3* gene, resulting in loss of functional caspase-3 expression, which blunts classical executioner caspase-dependent apoptotic pathways[25]. Furthermore, elevated intracellular glutathione (GSH) levels in MCF-7 cells enhance ROS-scavenging capacity, conferring relative resistance to oxidative cytotoxins compared with HeLa cells. T47D cells express functional caspase-3 but exhibit intermediate antioxidant capacity and high anti-apoptotic Bcl-2 expression, resulting in cytotoxic sensitivity intermediate between that of HeLa and MCF-7 cell lines[26]. Overall, these findings confirm that continuous-flow-synthesized cinnamaldehyde and ethyl cinnamate exert selective, ROS-mediated antiproliferative effects governed by cancer cell-specific apoptotic profiles.

CONCLUSION

This study demonstrates that microflow reactor technology provides an efficient, rapid, and highly controlled platform for the continuous synthesis of cinnamaldehyde and its ester derivative, ethyl cinnamate. The optimized microfluidic process achieved cinnamaldehyde with 100% relative chromatographic purity and a 52% isolated yield within a 10-minute residence time at 70°C, while the subsequent two-step sequence successfully yielded ethyl cinnamate at 99% purity. Biological evaluation revealed that cinnamaldehyde possessed superior cytotoxic potential compared to ethyl cinnamate across all tested cancer cell lines, exhibiting the highest potency against HeLa cervical carcinoma cells (IC_{50} = 95 µg/mL). This differential activity underscores the critical pharmacophoric role of the conjugated aldehyde moiety, relative to the ester derivative, in driving inhibition of cell growth. Nevertheless, because the synthesized compounds demonstrated lower antiproliferative potency than the commercial cinnamaldehyde standard (IC_{50} = 1.56 µg/mL) and the reference chemotherapeutic doxorubicin (IC_{50} = 0.14 µg/mL), future research should focus on further structural optimization and chemical derivatization to enhance their therapeutic efficacy as potential anticancer agents.

ACKNOWLEDGMENT

This research received financial support from the Ministry of Higher Education, Science, and Technology, through the Directorate of Research and Community Service, under the Regular Fundamental Research Program for Fiscal Year 2025. The authors express their sincere appreciation for this financial support. Gratitude is also extended to the Department of Chemistry at Institut Teknologi Bandung for providing NMR analytical facilities, and to Universitas Muhammadiyah Surakarta for granting institutional facilities, laboratory infrastructure, and a supportive research environment that enabled the successful execution of this study.

AUTHORS' CONTRIBUTION

Conceptualization: Muhtadi, Andi Suhendi, Ahmad Fauzi, Didin Mujahidin, Ahwan, Agustono Wibowo
Data curation: Nindita Fransiska Rahmawati, Muhtadi, Andi Suhendi, Ahmad Fauzi
Formal analysis: Muhtadi, Andi Suhendi, Ahmad Fauzi, Didin Mujahidin, Ahwan, Agustono Wibowo
Funding acquisition: Muhtadi
Investigation: Nindita Fransiska Rahmawati, Muhtadi, Andi Suhendi, Ahmad Fauzi
Methodology: Muhtadi, Andi Suhendi, Ahmad Fauzi, Didin Mujahidin
Project administration: Muhtadi
Resources: Muhtadi, Andi Suhendi, Ahmad Fauzi, Didin Mujahidin
Software: -
Supervision: Muhtadi, Didin Mujahidin
Validation: Muhtadi, Andi Suhendi, Ahmad Fauzi, Didin Mujahidin, Ahwan, Agustono Wibowo

Visualization: -
Writing - original draft: Nindita Fransiska Rahmawati, Muhtadi, Andi Suhendi, Ahmad Fauzi, Didin Mujahidin, Ahwan
Writing - review & editing: Muhtadi, Andi Suhendi, Ahmad Fauzi, Didin Mujahidin, Ahwan, Agustono Wibowo

DATA AVAILABILITY

None.

CONFLICT OF INTEREST

The authors declared no conflict of interest.

REFERENCES

1. Jimenez BAJ, Awwad F, Desgagné-Penix I. Cinnamaldehyde in Focus: Antimicrobial Properties, Biosynthetic Pathway, and Industrial Applications. Antibiotics. 2024;13(11):1095. DOI: 10.3390/antibiotics13111095; PMID: 39596788; PMCID: PMC11590939.

2. Zhang G, Li T, Liu J, Wu X, Yi H. Cinnamaldehyde-Contained Polymers and Their Biomedical Applications. Polymers. 2023;15(6):1517. DOI: 10.3390/polym15061517; PMID: 36987298; PMCID: PMC10051895.

3. Guo J, Yan S, Jiang X, Su Z, Zhang F, Xie J, et al. Advances in pharmacological effects and mechanism of action of cinnamaldehyde. Front Pharmacol. 2024;15:1365949. DOI: 10.3389/fphar.2024.1365949; PMID: 38903995; PMCID: PMC11187351.

4. Handayani A, Lailaty IQ, Rosyidah A, Sari DRT, Yunarto N, Suherman D. Indonesian Cinnamon (Cinnamomum burmanni (Nees & T. Nees) Blume) as Promising Medicinal Resources: A Review. J Sylva Lestari. 2024;12(3):610-33. DOI: 10.23960/jsl.v12i3.929.

5. Fanelli F, Parisi G, Degennaro L, Luisi R. Contribution of microreactor technology and flow chemistry to the development of green and sustainable synthesis. Beilstein J Org Chem. 2017;13:520-42. DOI: 10.3762/bjoc.13.51; PMID: 28405232; PMCID: PMC5372749.

6. Capaldo L, Wen Z, Noël T. A field guide to flow chemistry for synthetic organic chemists. Chem Sci. 2023;14(16):4230-47. DOI: 10.1039/d3sc00992k; PMID: 37123197; PMCID: PMC10132167.

7. Jung J, Kaiser L, Deigner HP, Schmidt MS. Continuous synthesis of bromoalkyl glycosides by Fischer glycosylation in a microreactor. J Flow Chem. 2022;12:9-15. DOI: 10.1007/s41981-021-00202-0.

8. Richmond HH, inventor. Uniroyal Inc, assigne. Preparation of cinnamaldehyde. United States Patent US2529186A. 1950-11-07.

9. Foudah AI, Shakeel F, Alqarni MH, Ross SA, Salkini MA, Alam P. Simultaneous Estimation of Cinnamaldehyde and Eugenol in Essential Oils and Traditional and Ultrasound-Assisted Extracts of Different Species of Cinnamon Using a Sustainable/Green HPTLC Technique. Molecules. 2021;26(7):2054. DOI: 10.3390/molecules26072054; PMID: 33916710; PMCID: PMC8038348.

10. Puspita OE, Ihsan BRP, Saraswati A. Analytical method validation of cinnamaldehyde content in cinnamon (Cinnamomum burmannii) extract using high-performance liquid chromatography. J Med Pharm Allied Sci. 2023;12(4):5976–82. DOI: 10.55522/jmpas.V12I4.5005.

11. Amalia D, Ngadwiyana, Fachriyah E. Sintesis Etil Sinamat dari Sinamaldehid pada Minyak Kayu Manis (Cinnamomum cassia) dan Uji Aktivitas sebagai Antidiabetes. J Sains Mat. 2013;21(4):108-13.

12. Fadl F, Abdalla S, Ishaq A, Umar Y. DFT Study of the Molecular Structure, Conformational Preference, Spectroscopic and Vibrational Analysis of Cinnamic Acid and Cinnamaldehyde. J Mex Chem Soc. 2022;66(4):543–59. DOI: 10.29356/jmcs.v66i4.1757.

13. Purwaningsih Y, Syukur M, Purwanto URE. Sonochemical Synthesis of Ethyl Cinnamate. JKPK J Kimia Pendidikan Kimia). 2020;5(1):1-7. DOI: 10.20961/jkpk.v5i1.35525.

14. Singh N, Yadav SS, Kumar S, Narasihman B, Ramasamy K, Lim SM, et al. Synthesis, characterization, in-vitro and in-silico therapeutic studies of cinnamaldehyde derivatives. J Mol Struct. 2025;1321:140165. DOI: 10.1016/j.molstruc.2024.140165.

15. Dalcanale E, Montanari F. Selective Oxidation of Aldehydes to Carboxylic Acids with Sodium Chlorite-Hydrogen Peroxide. Chem Informationsdienst. 1986;17(34):198634147. DOI: 10.1002/chin.198634147.

16. Hussein AA, Al-Hadedi AAM, Mahrath AJ, Moustafa GAI, Almalki FA, Alqahtani A, Shityakov S, Algazally ME. Mechanistic investigations on Pinnick oxidation: a density functional theory study. R Soc Open Sci. 2020;7(2):191568. DOI: 10.1098/rsos.191568; PMID: 32257322; PMCID: PMC7062072.

17. Yu C, Li YL, Liang M, Dai SY, Ma L, Li WG, et al. Characteristics and hazards of the cinnamaldehyde oxidation process. RSC Adv. 2020;10(32):19124-33. DOI: 10.1039/c9ra10820c; PMID: 35518288; PMCID: PMC9053951.

18. Durndell LJ, Cucuzzella C, Parlett CMA, Isaacs MA, Wilson K, Lee AF. Platinum catalysed aerobic selective oxidation of cinnamaldehyde to cinnamic acid. Catal Today. 2019;333:161–8. DOI: 10.1016/j.cattod.2018.02.052.

19. Aztatzi-Mendoza MA, Porras-Núñez EL, Rivas-Galindo VM, Carranza-Rosales P, Carranza-Torres IE, García-Vielma C, et al. Green synthesis of ethyl cinnamates under microwave irradiation: photophysical properties, cytotoxicity, and cell bioimaging. RSC Adv. 2024;14(4):2391-401. DOI: 10.1039/d3ra06443c; PMID: 38213976; PMCID: PMC10783162.

20. Araújo MO, Pérez-Castillo Y, Oliveira LHG, Nunes FC, Sousa DP. Larvicidal Activity of Cinnamic Acid Derivatives: Investigating Alternative Products for Aedes aegypti L. Control. Molecules. 2020;26(1):61. DOI: 10.3390/molecules26010061; PMID: 33374484; PMCID: PMC7796249.

21. Kciuk M, Gielecińska A, Mujwar S, Kołat D, Kałuzińska-Kołat Ż, Celik I, et al. Doxorubicin-An Agent with Multiple Mechanisms of Anticancer Activity. Cells. 2023;12(4):659. DOI: 10.3390/cells12040659; PMID: 36831326; PMCID: PMC9954613.

22. Ka H, Park HJ, Jung HJ, Choi JW, Cho KS, Ha J, et al. Cinnamaldehyde induces apoptosis by ROS-mediated mitochondrial permeability transition in human promyelocytic leukemia HL-60 cells. Cancer Lett. 2003;196(2):143-52. DOI: 10.1016/s0304-3835(03)00238-6; PMID: 12860272.

23. Ranjitkar S, Zhang D, Sun F, Salman S, He W, Venkitanarayanan K, et al. Cytotoxic effects on cancerous and non-cancerous cells of trans-cinnamaldehyde, carvacrol, and eugenol. Sci Rep. 2021;11(1):16281. DOI: 10.1038/s41598-021-95394-9; PMID: 34381064; PMCID: PMC8358038.

24. Peng J, Song X, Yu W, Pan Y, Zhang Y, Jian H, et al. The role and mechanism of cinnamaldehyde in cancer. J Food Drug Anal. 2024;32(2):140-54. DOI: 10.38212/2224-6614.3502; PMID: 38934689; PMCID: PMC11210466.

25. Wang S, He M, Li L, Liang Z, Zou Z, Tao A. Cell-in-Cell Death Is Not Restricted by Caspase-3 Deficiency in MCF-7 Cells. J Breast Cancer. 2016;19(3):231-41. DOI: 10.4048/jbc.2016.19.3.231; PMID: 27721872; PMCID: PMC5053307.

26. Theodossiou TA, Olsen CE, Jonsson M, Kubin A, Hothersall JS, Berg K. The diverse roles of glutathione-associated cell resistance against hypericin photodynamic therapy. Redox Biol. 2017;12:191-7. DOI: 10.1016/j.redox.2017.02.018; PMID: 28254657; PMCID: PMC5333531.